# A FAST AND ROBUST ODF ESTIMATION ALGORITHM IN Q-BALL IMAGING

*Maxime Descoteaux*[†]*, Elaine Angelino*[§]

[†]Odyssee Team
INRIA Sophia Antipolis, France

*Shaun Fitzgibbons*[§]*, Rachid Deriche*[†*]

[§]Harvard University

## ABSTRACT

We propose a simple and straightforward analytic solution for the Q-ball reconstruction of the diffusion orientation distribution function (ODF) of the underlying fiber population. First, the signal is modeled with a high order spherical harmonic series using a Laplace-Beltrami regularization method which leads to an elegant mathematical simplification of the Funk-Radon transform using the Funk-Hecke formula. In doing so, we obtain a fast and robust model-free ODF approximation. We validate the accuracy of the estimation quantitatively against synthetic data generated from the multi-tensor model and show that our estimated ODF can recover known multiple fiber regions in a biological phantom and in the human brain.

## 1. INTRODUCTION

To resolve the well-known limitations of diffusion tensor imaging (DTI), recent research has been done to generalize the existing Gaussian diffusion model [1] with new higher resolution diffusion MRI acquisition techniques such as Q-Space Imaging (QSI) and High Angular Resolution Diffusion Imaging (HARDI). Stejskal and Tanner [2] showed that with the narrow pulse assumption, the signal attenuation $S(\mathbf{q})$ can be expressed as the 3D Fourier transform $\mathcal{F}$ of the ensemble average propagator $P$,

$$\frac{S(\mathbf{q})}{S_0} = \int P(\mathbf{r}) e^{-2\pi i \mathbf{q}^T \mathbf{r}} d\mathbf{r} = \mathcal{F}[P(\mathbf{r})], \qquad (1)$$

where the $\mathbf{q}$-value is an imaging parameter, $S_0$ is the baseline image and $P(\mathbf{r})$ is the probability that a spin starting at a given point in the voxel will have displaced by some radial vector $\mathbf{r}$ in the gradient pulse time. The latter is the probability density function (PDF) that characterizes the average diffusion of water molecules.

*This work has been partly supported by NSERC, the INRIA-FQRNT grant, the INRIA Internship program of the DREI Department and the National project "Large Dataset ACI Obs-Cerv". The authors would like to thank the McConnel Brain Imaging Center and J. Campbell, K. Siddiqi, V.V. Rymar and B. Pike for the rat dataset. Moreover, thanks to S. Lehéricy and K. Ugurbil at the Center for Magnetic Resonance Research for the human brain dataset. Finally, thanks to M. de La Gorce and C. Lenglet for their valuable inputs in this work.

Existing high order techniques generally approximate this PDF or variants of it such as the persistent angular structure (PAS), the fiber orientation distribution (FOD) or the diffusion orientation distribution function (ODF) which are very well reviewed in [3]. For all these functions, the important property is that their maxima agree with the underlying fiber orientations. However, these existing methods lack a straightforward regularization process and are all computed numerically which is computationally expensive. In this paper, we overcome these limitations by proposing a closed form for the Funk-Radon transform that estimates the ODF. It is based on a physically meaningful regularized spherical harmonic series approximation of the measured signal which is simple and fast to compute.

## 2. Q-BALL IMAGING

Q-ball Imaging (QBI) [4] seeks to reconstruct the diffusion ODF. The latter is intuitive and gives a good representation of the underlying fiber distribution which as made it a popular tool in many high order recent works for fiber tracking [5, refs. therein]. The ODF in a unit direction $\mathbf{u}$ is given by the radial projection of the diffusion PDF and without lost of generality, if $\mathbf{u}$ is the z-axis, the exact ODF can be expressed as

$$\Psi(\mathbf{u}) = \int_0^\infty P(\alpha \mathbf{u}) d\alpha = \int P(r,\theta,z)\delta(\theta,z) r dr d\theta dz. \qquad (2)$$

Tuch [4] showed that this ODF could be estimated directly from the raw HARDI data on a single sphere of q-space by the Funk-Radon transform (FRT) $\mathcal{G}$ by proving that

$$\mathcal{G}_{q'}[S(\mathbf{q})](\mathbf{u}) = 2\pi q' \int P(r,\theta,z) J_0(2\pi q' r) r dr d\theta dz, \quad (3)$$

which is essentially a smoothed version of the true ODF of Eq. 2. In fact, the larger the $q'$, the closer the FRT approximation is to the exact ODF as the zeroth-order Bessel function $J_0$ approaches a Dirac delta function $\delta$. In practice, the FRT value at a given spherical point $\mathbf{u}$ is the great circle integral of the signal on the sphere defined by the plane through the origin with normal vector $\mathbf{u}$. A matrix multiplication can implement this integral but involves several numerical computations such as a regridding to find points outside the ac-

tual measurements required to compute the discrete points on each great circle [4, tbl.1]. Our main contribution in this article is to show how to solve this FRT integral analytically by first showing how to find a regularized spherical harmonics parametrization of the input signal.

## 3. A NEW ODF ESTIMATION

### 3.1. Signal Description Using Spherical Harmonics

The spherical harmonics (SH), normally indicated by $Y_\ell^m$ ($\ell$ denotes the order and $m$ the phase factor), are a basis for complex functions on the unit sphere. Letting $j = (\ell, m)$, we showed in [6] how to define a new modified SH basis, $Y_j$, designed to be *symmetric*, *orthonormal* and *real*. The latter better models the physical constraints of the diffusion MRI acquisition. We can thus approximate the diffusion signal at each of the $n_s$ gradient direction $i$ as

$$S(\theta_i, \phi_i) = \sum_{j=1}^{N} c_j Y_j(\theta_i, \phi_i) \tag{4}$$

where $N = (\ell + 1)(\ell + 2)/2$ is the number of terms in the SH series of order $\ell$. We can write the set of equations as an over-determined linear system $S = BC+$error, where B is constructed with the modified spherical harmonics basis

$$B = \begin{bmatrix} Y_1(\theta_1, \phi_1) & \cdots & Y_N(\theta_1, \phi_1) \\ \vdots & \ddots & \vdots \\ Y_1(\theta_{n_s}, \phi_{n_s}) & \cdots & Y_N(\theta_{n_s}, \phi_{n_s}) \end{bmatrix}$$

and C is the vector of SH coefficients $c_j$. We want to solve for $C$, where $c_j = \int_\Omega S(\theta_i, \phi_i) Y_j(\theta_i, \phi_i) d\Omega$, where integration over $\Omega$ denotes integration over the unit sphere. At this point, instead of evaluating the integrals directly [7] or performing a simple least-squared minimization as in [8], we add local regularization to our fitting procedure. We define a measure of the deviation from smoothness $E$ of a function $f$ defined on the unit sphere as $E(f) = \int_\Omega (\triangle_b f)^2 d\Omega$, where $\triangle_b$ is the Laplace-Beltrami operator. The Laplace-Beltrami operator, which is the Laplacian operator in spherical coordinates, is a natural measure of smoothness for functions defined on the unit sphere. It has a very simple expression as it must satisfy the relation $\triangle_b Y_j = -\ell_j(\ell_j + 1) Y_j$. As a result, using the orthornormality of the modified SH basis, the above functional $E$ can be rewritten straightforwardly as

$$\begin{aligned} E(f) &= \int_\Omega \triangle_b \left( \sum_p c_p Y_p \right) \triangle_b \left( \sum_q c_q Y_q \right) d\Omega \\ &= \sum_{j=1}^{N} c_j^2 \ell_j^2 (\ell_j + 1)^2 = C^T \mathbf{L} C, \end{aligned} \tag{5}$$

where L is simply the square matrix with entries $\ell_j^2(\ell_j + 1)^2$ along the diagonal. Therefore, the quantity we wish to minimize can be expressed in matrix form as $M(C) = (BC - S)^T (BC - S) + \lambda C^T L C$, where $\lambda$ is the weight on the regularization term. The coefficient vector minimizing this expression can then be determined just as in the standard least-squares fit ($\lambda = 0$), from which we obtain the generalized closed form expression for the desired spherical harmonic series coefficient vector

$$\boxed{C = (B^T B + \lambda L)^{-1} B^T S} \tag{6}$$

From this SH coefficient vector we can recover the signal on the Q-ball for any $(\theta, \phi)$ as $S(\theta, \phi) = \sum_{j=1}^{N} c_j Y_j(\theta, \phi)$. Intuitively, this approach penalizes an approximation function for having higher order terms in its modified SH series. Therefore, higher order terms will only be included in the fit if they significantly improve the overall accuracy of the approximation. This eliminates most of the high order terms due to noise while leaving those that are necessary to describe the underlying function. However, obtaining this balance depends on choosing a good value for the parameter $\lambda$. We use the *L-curve* numerical method to determine the best $\lambda$. [6, 9].

### 3.2. Analytic Funk-Radon Transform

The Funk-Hecke theorem [10] is a powerful formula that relates the inner product of any surface harmonic with the projection on the sphere of any continuous function defined on the interval $[-1, 1]$.

> **Funk-Hecke Theorem:** Let f(t) be continuous on $[-1, 1]$ and $H_\ell$ any surface harmonic of order $\ell$. Then, given a unit vector $\mathbf{x}$
>
> $$\int_{|\mathbf{u}|=1} f(\mathbf{x}^T \mathbf{u}) H_\ell(\mathbf{u}) d\mathbf{u} = \lambda(\ell) H_\ell(\mathbf{x}), \tag{7}$$
>
> where
>
> $$\lambda(\ell) = \frac{2\pi}{P_\ell(1)} \int_{-1}^{1} P_\ell(t) f(t) dt$$
>
> with $P_\ell$ the Legendre polynomial of degree $\ell$.

We use the theorem to evaluate the Funk-Radon integral. By replacing the signal with our series of SH, the FRT in a unit direction $\mathbf{x}$ can be expressed as

$$\begin{aligned} \mathcal{G}[S](\mathbf{x}) &= \int_{|\mathbf{u}|=1} \delta(\mathbf{x}^T \mathbf{u}) S(\mathbf{u}) d\mathbf{u} \\ &= \sum_j c_j \underbrace{\int_{|\mathbf{u}|=1} \delta(\mathbf{x}^T \mathbf{u}) Y_j(\mathbf{u}) d\mathbf{u}}_{I} \end{aligned} \tag{8}$$

Note that if the Dirac delta function $\delta$ were continuous on the interval $[-1, 1]$, $I$ could be directly evaluated using the Funk-Hecke formula of Eq. 7. However, $\delta(t)$ is discontinuous at zero. Hence, we approximate the Dirac delta function with a Gaussian of decreasing variance given by $\delta_n(x) =$

$(n/\sqrt{\pi})e^{-n^2x^2}$. This is a well-known delta sequence which converges to a Dirac delta function ($\lim_{n\to\infty}\delta_n = \delta$), i.e.

$$\lim_{n\to\infty}\int_{-\infty}^{\infty}\delta_n(x)f(x) \quad = \quad f(0). \tag{9}$$

Since the Gaussian is continuous on the interval $[-1,1]$, the delta sequence $\delta_n$ is also continuous on $[-1,1]$ for all $n$. Hence,

$$\begin{aligned} I(\mathbf{x}) &= \int \delta(\mathbf{x}^T\mathbf{u})Y_j(\mathbf{u})d\mathbf{u} \\ &= \lim_{n\to\infty}\int \delta_n(\mathbf{x}^T\mathbf{u})Y_j(\mathbf{u})d\mathbf{u} \\ &= \frac{2\pi}{P_\ell(1)}\left(\lim_{n\to\infty}\int_{-1}^{1}\delta_n(t)P_\ell(t)dt\right)Y_j(\mathbf{x}) \quad \text{(Eq. 7)} \\ &= 2\pi\frac{P_{\ell_j}(0)}{P_{\ell_j}(1)}Y_j(\mathbf{x}) \quad \text{(Eq. 9)} \end{aligned}$$

Therefore, referring back to Eq. 8, the FRT of a function given in terms of our modified spherical harmonic series is

$$\mathcal{G}[S(\mathbf{q})](\mathbf{x}) = \sum_j 2\pi\frac{P_{\ell_j}(0)}{P_{\ell_j}(1)}c_jY_j(\mathbf{x}) \tag{10}$$

Thus, the spherical harmonics are eigenfunctions of the Funk-Radon transform with eigenvalues depending only on the order $\ell$ of the SH series. When the signal $S(\mathbf{q})$ is parametrized by the vector $C$ of SH coefficients, i.e. $S = BC$, the analytic Funk-Radon transform for all directions is obtained in a single step with a diagonal linear transformation given by

$$ODF \approx \begin{pmatrix} \ddots & & \\ & 2\pi\frac{P_{\ell(j)}(0)}{P_{\ell(j)}(1)} & \\ & & \ddots \end{pmatrix}\begin{pmatrix} \vdots \\ c_j \\ \vdots \end{pmatrix} = PC \tag{11}$$

Hence, not only do spherical harmonics allow the definition of a simple regularization procedure but also simplify greatly the computation of the FRT using the Funk-Hecke formula.

## 4. EVALUATING THE ODF ESTIMATION

We now evaluate our ODF estimation. We use the multi-tensor model [8, 6] because it is simple and it leads to an analytic computation of the exact ODF. The exact ODF is given in Tuch [4, Eq.2] for a single Gaussian fiber and by linearity, we can easily obtain the exact ODF for many fibers. Hence, we generate a set of 1000 mixed random 1, 2 and 3 fiber distributions using a HARDI sampling of 81 gradient direction on the hemisphere with different $b$-values, different noise levels, random angles between fibers and random relative fiber weights, each time calculating the optimal regularization $\lambda$ parameter. We use an order-8 SH approximation of the signal to obtain the coefficients $C$ given by Eq. 6 and then apply the linear transformation $P$ given Eq. 11 to obtain the estimated ODF, $f'$.

Letting $f$ represent the exact ODF for the fiber distribution, we can compute a simple Euclidean average of the squared error between $f$ and $f'$ over all $n_s$ gradient sampling on the sphere as $[f,f'] = 1/n_s\sum_{i=1}^{n_s}(f'_i - f_i)^2$. Moreover, we can compute another interesting comparison measure if we also describe $f$ with an order-8 SH series. Although this last step is not exact, it also leads to a very simple expression of the inner product between the two functions on the sphere. Recalling the real and orthonormality of our modified SH basis, the inner product is $< f, f' >= \int_\Omega f\cdot f' d\Omega = \sum_j c_j\cdot d_j$, which is $C^TD$ in matrix form when $C$ and $D$ are the respective vectors of SH coefficients of $f$ and $f'$. If we normalize such that $< f, f >=< f', f' >= 1$, this angularity measure is 1 when the functions are the same and its range is $[-1,1]$.

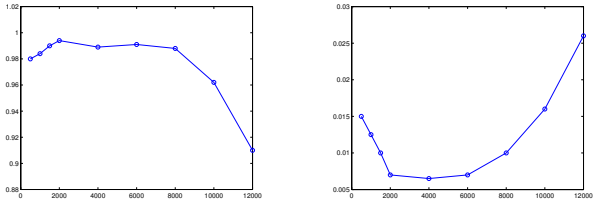

$< f, f' >$ vs. $b$-value $\qquad$ $[f, f']$ vs. b-value

**Fig. 1**. Highest accuracy and lowest error are respectively observed for a plateau of high $b$-values between 2000 and 6000.

As seen in Fig.1, the estimation is very precise and we observe the same behavior using both angularity measure for comparison. As expected, the accuracy using the inner product is $> 0.99$ and the Euclidean average normalized error is $< 0.01$ for a plateau of relatively high $b$-values between 2000 and 6000. Note also that for low $b$-values, the Bessel function averaging effect mentioned earlier reduces the precision of the estimation. Finally, observe that the best results are not necessarily for very high $b$-values because in this case, the signal is sharper and the effect of noise more important.

Finally, we illustrate how the estimated ODF are able to recover voxels with multiple fibers. The ODFs are overlaid on the Generalized Fractional Anisotropy (GFA) measure [4] with the maxima detected. First, we show the recovered crossings in the rat spinal chords phantom Fig.2 created by Campbell et al. [5] at the Montreal Neurological Institute. This data was acquired on a 1.5 Tesla scanner with 90 gradient directions and a $b$-value of 3000. Note that the DTI ellipsoids cannot distinguish the multiple directions. We can also recover known multi-fiber voxels in the human brain. This dataset was acquired on a 3 Tesla scanner, has 3mm$^3$ cubic grid and contains 24, 64x64 slices with 81 gradients and a $b$-value of 1000. Fig.3 high-lights two important crossings in the central semiovale. First, the corona radiata crossing the corpus callosum (cc) transcallosal fibers projecting to the precentral gyrus. Secondly, the crossings between transcallosal projections and superior longitudinal fasciculus (sfl), which are ro-

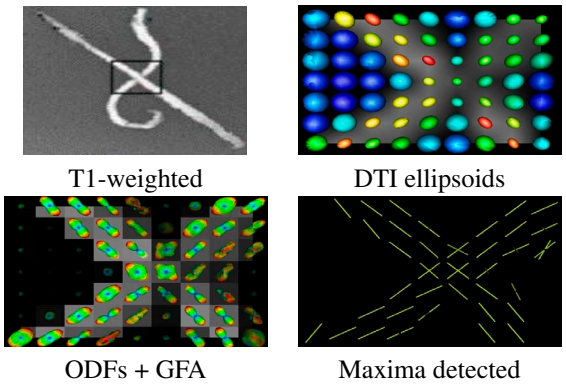


**Fig. 2**. ODFs for the rat biological phantom from [5].

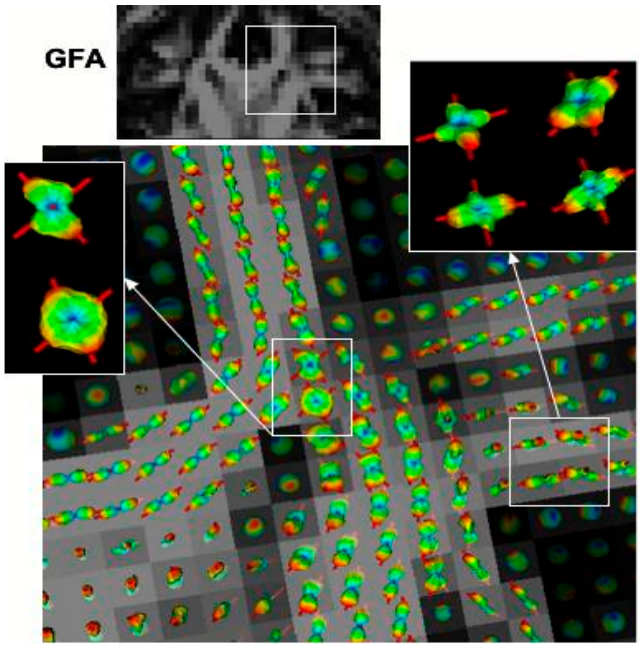


**Fig. 3**. Coronal slice with multiple fiber crossings.

tated by ninety degrees in the zoomed version to facilitate the visualization of the slf fibers coming out of the page. Note also the single fibers of the body of the cc coming out of the page in the lower left corner.

## 5. DISCUSSION AND CONCLUSION

The principal contribution of this paper is the derivation of an analytic solution of the Funk-Radon transform (FRT) commonly solved numerically in Q-ball imaging to reconstruct the orientation density function (ODF). This was possible using a physically meaningful regularized spherical harmonics approximation of the measured signal. The final ODF estimation is an elegant product of the modified SH basis function with the simple ratio of the corresponding order-$\ell$ Legendre polynomials evaluated at 0 and at 1. This simplification was possible by using a delta sequence so that the Funk-Hecke formula could be used to solve the Funk-Radon integral. Without this derivation, the FRT can only be computed with a more complicated numerical scheme. Assuming, the multi-tensor model, we have shown that the ODF estimation is very accurate and behaves as expected. Finally, it is clear that multiple fiber distributions can be detected from noisy sparse real HARDI as demonstrated on a biological phantom and regions of the human brain.

## 6. REFERENCES

[1] P.j. Basser, J. Mattiello, and D. LeBihan, "MR diffusion tensor spectroscopy and imaging," *Biophysical Journal*, , no. 66, pp. 259–267, 1994.

[2] E.O. Stejskal and J.E. Tanner, "Spin diffusion measurements: spin echoes in the presence of a time-dependent field gradient," *Journal of Chemical Physics*, vol. 42, pp. 288–292, 1965.

[3] D.C. Alexander, "Multiple-fibre reconstruction algorithms for diffusion mri," *Annals of the New York Academy of Sciences*, 2005, in press.

[4] D. Tuch, "Q-ball imaging," *Journal of Magnetic Resonance in Medicine*, vol. 52, pp. 1358–1372, 2004.

[5] S.W. Campbell, K. Siddiqi, V.V. Rymar, A.F. Sadikot, and G.B. Pike, "Flow-based fiber tracking with diffusion tensor q-ball data: Validation and comparison to principal diffusion direction techniques," *NeuroImage*, vol. 27, no. 4, pp. 725–736, Oct. 2005.

[6] M. Descoteaux, E. Angelino, S. Fitzgibbons, and R. Deriche, "Apparent diffusion coefficients from high angular resolution diffusion imaging: Estimation and applications," Tech. Rep. 5681, INRIA, Sept. 2005.

[7] L.R. Frank, "Characterization of anisotropy in high angular resolution diffusion-weighted mri," *Magn. Res. Med*, vol. 47, pp. 1083–1099, 2002.

[8] D.C. Alexander, G.J. Barker, and S.R. Arridge, "Detection and modeling of non-gaussian apparent diffusion coefficient profiles in human brain data," *Journal of Magnetic Resonance in Medicine*, vol. 48, pp. 331–340, 2002.

[9] P.C. Hansen, "The l-curve and its use in the numerical treatment of inverse problems," in *Computational Inverse Problems in Electrocardiology,*, P. Johnston, Ed., 2001, pp. 119–142.

[10] G.E. Andrews, R. Askey, and R. Roy, *Special Functions*, Cambridge University Press, 1999.